Hybridization between deep learning algorithms and neutrosophic theory in medical image processing: A survey

NN Mostafa [1], K Ahmed[2], and I El-Henawy [3]

[1]   Computer Science Department, Zagazig University, Zagazig, Egypt; nihal.nabil@fci.zu.edu.eg
[2]   Computer Science Department, Beni-Suef University, Beni Suef, Egypt;kareem_ahmed@eng.bsu.edu.eg
[3]   Computer Science Department, Zagazig University, Zagazig, Egypt; henawy2000@yahoo.com.

Abstract: Deep learning can successfully extract data features based on dealing greatly with non-linear problems. Deep learning has the highest performance in medical image analysis and diagnosis. Additionally, deep learning performance is affected by insufficient medical image data such as fuzziness or incompleteness. The neutrosophic approach can enhance deep learning performance with its great dealing with inconsistency and ambiguity information in medical data. This survey investigates the various ways in which deep learning is enhanced with neutrosophic systems and provides an overview and concept on each other. The hybrid techniques are classified based on different medical image modalities in different medical image processing stages such as preprocessing, segmentation, classification, and clustering. Finally, future works are also explored. In this study the highest accuracy was achieved by hybridization between neutrosophic and LASTM to classify the cardio views. While the highest capability to precisely detect those with the disease (sensitivity) is achieved by integration between neutrosophic, convolution neural network and support vector machine. Best specificity was obtained by neutrosophic and LSTM.

Keywords: Medical image; Neutrosophic; Deep learning; denoising; classification; segmentation; clustering; image modalities.

1. Introduction

Recently, rapid diagnosis, and treatment of diseases becomes a major area in computer science using different medical image modalities such as computed tomography (CT), magnetic resonance imaging (MRI), Microscopic image analysis (MIA), ultrasound (US), and X-ray [1]. Usually, radiologists and physicians perform the interpretation of a medical image. However, Computer-aided systems can help human experts and doctors from potential fatigue and individual variations in pathology reading. Deep learning (DL) and neutrosophic techniques can help to improve the rate of computational medical image analysis [2].

In the last few decades, many automatic analysis systems have been implemented from scanned and loaded medical images. Between the 1970s and 1990s, low-level pixel and mathematical processing (edge detection, region growing, fitting lines) were the main techniques for doing medical image analysis. It was common in that period there are same as if-then-else statements in expert systems. Haugeland, 1985 named these systems GOFAI (good old-fashioned artificial intelligence) like rule-based image processing systems [3, 4].

Supervised learning (SL) develops systems using training data at the end of the 1990s. These systems become more and more common in medical image analysis such as atlas approaches which fit new data from the training data, feature extraction, and use of statistical classifiers such as

computer-aided diagnosis (CAD) and active shape models. These methods have become successful in many medical image analysis tasks. So, systems are trained using extracted data vectors instead of data designed by humans. The optimal decision boundary is done using computer algorithms in high dimensional space. Feature extraction is a vital step in model deployment. This process is named the hand-crafted feature [4].

Logical progress is learning optimal features that represent data for a complex problem. This concept lies at the foundation of many DL models. So, DL techniques permit the machine to make data interpretation by learning complex mathematical problems. These models consist of linear and/or non-linear functions as input data and weighted model parameters. These functions treat hierarchy as a layer, so the name of DL is inspired by a larger number of such layers. Usually, Training data tasks such as denoising, segmentation, and classification help the computational model to learn its parameter. The basic idea of DL is an Artificial Neural Network (ANN) that contains multiple layers of neurons, while its parameters (weights) identify the parameter of the connections between the neurons and layers [5].

DL uses testing data to perform the same task accurately, which makes DL more generalizable than other different machine learning (ML) techniques. DL learn parameter using a back-propagation strategy which iteratively attains the desired parameter value using the Gradient Descent technique. The single epoch is the terminology of update the model parameter using whole training data once. Usually, modern DL models are trained for hundreds of epochs before utilization [5].

Convolutional neural networks (CNNs) are the most popular network in DL. A CNN does a mathematical operation called convolution [6]. CNN was introduces to the world in handwriting digit recognition in LeNet [7]. After those novel approaches were implemented for effectively training deep networks, and improvements were produced in main computing systems. Krizhevsky et al. (2012) proposed the AlexNet based on CNNs which trained on ImageNet data in December 2012 [8].

The medical image analysis society observes these crucial improvements. later than, other DL architecture has deployed recurrent neural networks (RNNs), autoencoders (AEs), restricted Boltzmann machines (RBMs) [9], and deep belief networks (DBN). All these contributions take attention to the medical image analysis community [4].

On the other hand, many problems in medical image analysis have been shown such as impression and uncertainty, incomplete, fuzziness, and inconsistent, which derive from acquisition errors, incomplete knowledge, or stochasticity. These problems make denoising, segmentation, clustering, and classification are difficult operations to perform on medical image analysis [10]. So soft computing combined with medical applications and DL architecture to get solutions for unsolvable problems. Many theories can deal with ambiguous information such as para consistence logic theory [11], intuitionistic fuzzy set (IFS) theory [12], fuzzy set (FS) theory [13], probability theory [14]. One of these methods is the FS introduced by Zadeh (1965) which solves fuzziness and ambiguity problems that exist in medical data [15]. One disadvantage of FS that it doesn't take indeterminacy in its consideration independently [16].

Neutrosophy is a novel philosophy branch adopted by Smarandache that is a scope of neutralities. Neutrosophy can specify classical logic, fuzzy logic (FL), and imprecise probability. Human rational can deal with the ambiguity of knowledge linguistic mistakes and so neutrosophy can deal with this ambiguity. Usually, neutrosophy includes a neutrosophic set (NS) which can deal

with neutralities along with their relations. Neutrosophy has truth, falsity, and an indeterminacy degree, which are independent of each other [17].

Medical data is unpredictable, partial, inaccurate, incomplete, and vague. Expert systems vary in inputs because of not existence of the specified policy in treatment or drug usage. Normally, a large scale of information process is needed in a medical image, a significant part is unconscious and rapid processing and computation. Therefore, indeterminacy, irregularity, ambiguities, and vagueness must be solved. Intelligent diagnosis system has been observed by computer science and applicable mathematics field. So evolutionary neural network in breast cancer detection has been proposed by [18]. Also, Tan et al. [19] classified the hepatitis rule and breast cancer cases using a hybrid evolutionary algorithm (EA) and genetic programming (GP).

A new neuro-fuzzy technique for segmentation of the MRI data to brain tumor [20]. Lately, NL and NS have major importance in medical applications. Neutrosophic systems prove its successful effect than fuzzy counterparts. It can deal with major processes in medical systems such as data acquisition, data generation, indeterminacy, truth, and falsity. Hence, NS comprises truth, indeterminate, and false membership functions. In2015, Ye [21] proposed the improved cosine similarity measure for simplified NS (SNS) and applied it to medical diagnosis. The single-valued NS (SVNS) is the crucial usage set in most applications introduced by Wang et al. [22].

There are lots of surveys in medical image analysis discuss the use of NS in different levels of image analysis such as (denoising, segmentation, and classification) or using NS in different medical image modalities on different organs, but all of these surveys did not cover the last researchs and algorithms of using DL under NS theory [23], [24], [25], [26], [27], [28], [29]. Also (Elhassouny et al.,2019) discuss the integration of NS and ML algorithms, but not cover the medical image analysis domain [30]. On the other hand, many surveys on DL in a medical image, but these studies ignore the dealing of inconsistency and fuzzification information in the medical image [2], [31], [4], [32].

This study aims to introduce a survey on DL algorithms in medical image processing under a NS theory. The following sections are arranged as follows. Section 2 provides an overview of different image modalities. Section 3 provides a general concept of NS and NS algorithms that are used in medical image processing stages such as denoising, segmentation, and classification in different image modalities such as MRI, CT, US, CT, and MIA. In section 4 we introduce an overview of the DL concept and previous work on techniques that commonly used different medical image processing stages. In section 5 explores hybridization between NS and DL and how this integration can affect the performance in medical image processing and analysis.

2. Medical image modalities

The medical image modalities help for more medical image analysis and diagnosis. Medical image modalities differ in characterization and applications that assist the study organs and diagnosis and treatment follow-up. These modalities can be categorized into five types: MIA, MRI, US, X-ray, CT [33]. A short discussion about these modalities is introduced in Table 1.

Table 1. Medical Imaging Modalities.

Medical image modalities	Famous issue
MIA	Fuzziness, inconsistency, weak robustness[29].

MRI	Gaussian, Rician, Rayleigh[27].
US	Gaussian, Speckle noise[27].
X-Ray	Gaussian, Poisson[34].
CT	Speckle noise, gaussian noise, salt and pepper noise[35].

2.1 Microscopic image analysis

MIA is a good effect on converting to completely automatic analysis instead of the human observer. MIA Can carry a blood smear or any tissue of the human body [36]. MIA can help improve the diagnosis performance in various diseases. Many applications use MIA in processing techniques such as image enhancement, microscopic segmentation, cell classification, and White blood cell detection.

2.2 Magnetic resonance imaging

MRI is essential in non-invasive diagnosis and is one of the most commonly and reliably used clinical situations. The most characterization of MRI that it can pick up soft tissue such as blood vessels, organs in the pelvis, the abdomen of (heart, liver, kidney). These cross-sectional images are taken by magnets and radio waves to form a slice of the human body.

MRI is safe for children and pregnant women because no radiation exposure also has high accuracy. On the other hand, MRI has a great sensitivity to a movement which affects the organs that involve movement. Additionally, MRI suffers from magnetic field distribution and patients cannot wear metallic devices such as pacemakers. Many applications of computer science using MRI such as tissue classification, liver diagnosis,3D tumor visualization [33].

2.3 Ultrasound

The US transformed the echoes retrieving sounds into images, So the US cannot detect bone organs. Advantage of US is low cost, high resolution, no radiation, and widely available scan. But it is difficult to image lungs and bones resolution to be affected easily. A lot of applications are using US images such as pregnancy, breast cancer detection, liver and tumor diagnosis [33].

2.4 X-ray image

X-rays are considered the most and oldest imaging types. X-ray images formed using electromagnetic radiation. Most X-ray applications are detecting problems with the skeletal system, diagnose cancer via mammography, gastric concerns, and dental problems detection [27].

2.5 Computed tomography

Series of Cross-sectional images are formed using x-ray sensors. So, it can detect hard tissue such as bones. CT has a wide scan area so it can pick up blood vessels and brain, liver. CT has an advantage over MRI in that it has a short time of scan with high resolution. But it has limitations in tissue characterization, sensitivity, high cost, and high radiation. Many applications are using the CT image such as covide-19 detection, chest diagnostic, brain simulation, tumor detection [33].

3. Neutrosophic set in medical image analysis

Samarandache introduced neutrosophic in 1995 which is the generalization form of fuzzy [37]. Neutrosophy is the fundamental of neutrosophic probability, neutrosophic statistics, neutrosophic logic (NL), and (NS) [37]. The NS is the general concept of the classical sets, FS, interval-valued fuzzy set [38], IFS [39]. NS concept (A) in relation to its opposite (Anti-A) and the neutrality (Neut-A), which is not (A) nor (Anti-A). The (Neut-A) and (Anti-A) are mentioned as (Non-A). So concept (A) is neutralized and balanced by (Anti-A) and (Non-A) concepts [40].

NL defines three neutrosophic components: T, I, F for truth, false, and indeterminacy membership degree in <A>.NL can handle the uncertainty by providing extra domain I which increases the efficiency of dealing with uncertainty unlike FL [41]. NL is able to perform the difference between relative truth and absolute truth as well as between relative falsity and absolute falsity, so NL component (T, I, F) can be over-flooded over 1 or under-dried 0 [23].Commonly, some definitions are given for the NS as follows: [40, 42]

Definition 1. T, I and F are real standard or non-standard of $]-0,1+[$ with

$$supT = t\_sup, infT = t\_inf,$$

$$supI = i - sup, infI = i_{inf}, supF = f_{sup}, infF = f_{infandn_{sup}} = t_{sup} + i_{sup} + f_{sup}, n_{inf} = t_{inf} + \cdots$$

$$i_{inf} + f\_inf$$

Definition 2. (Neutrosophic image) for U is universe, a neutrosophic image P_{NS} is characterized by subsets T, I and F. A pixel P in the image is defined as P(T, I,F).Then, the pixel P(n,m) in the image domain is converted to NS image using the following equations:

$$H_{NS}(n, m) = \{T(n, m), I(n, m), F(n, m)\} \qquad (1)$$

Where *T(n,m),I(n,m) and F(n,m)* probabilities of white, indeterminate, non-white sets:

$$T(n, m) = \frac{\bar{g}(n, m) - \bar{g}_{min}}{\bar{g}_{max} - \bar{g}_{min}} \qquad (2)$$

$$\bar{g}(n, m) = \frac{1}{w * w} \sum_{x=n-w/2}^{n+w/2} \sum_{y=m-w/2}^{m+w/2} g(x, y) \qquad (3)$$

$$I(n, m) = \frac{\delta(n, m) - \delta_{min}}{\delta_{max} - \delta_{min}} \qquad (4)$$

$$\delta(n, m) = abs(g(n, m) - \bar{g}(n, m)) \qquad (5)$$

$$F(n, m) = 1 - T(n, m) \qquad (6)$$

Where *g(n,m)* is the intensity value of the pixel (n, m) , $\bar{g}(n, m)$ is the local mean value of $g(n, m), \delta(n, m)$ is the absolute value of the difference between intensity $g(n, m)$ and its local mean value $\bar{g}(n, m)$ [23].

Definition 3. (Neutrosophic image entropy) The gray image entropy measures the distribution of intensities. Maximum entropy value implies for equal intensities probability and small entropy implies for non-uniform intensity distribution [23]. The NS image entropy defined as the summation of the entropies of three subsets T, I and F, which is given by:

$$E_{NS} = E_T + E_I + E_F \qquad (7)$$

$$E_T = - \sum_{i=\min\{T\}}^{\max\{T\}} P_T(i) \ln P_T(i) \qquad (8)$$

$$E_I = -\sum_{i=\min\{I\}}^{\max\{I\}} P_I(i) \ln P_I(i) \qquad (9)$$

$$E_F = -\sum_{i=min\{F\}}^{\max\{F\}} P_F(i) \ln P_F(i) \qquad (10)$$

where, E_T, E_I and E_F are the entropies of sets *T, I* and *F*, respectively. Also, $P_T(i), P_I(i), P_F(i)$ are the probabilities in *T, I* and *F*; respectively. Commonly, E_T and E_F are used to measure the distribution of the elements in NS, and E_I is evaluated to measure the indeterminacy distribution.

Recently NL and NS had major importance in the medical domains. Neutrosophic systems are noticed to be more successful than fuzzy systems. NS can deal with indeterminacy in medical information which makes it more generalization than FS [23]. NS provides approximate the connection between modern medical image analysis and fuzzy approaches. It improves performance in different medical systems processes such as acquisition, generation, sorting. Therefore, the NS has an independent (T, I, F) membership function. Lately, Ye [21] used the cosine function, SVNS, and interval neutrosophic cosine similarity to propose cosine similarity measures for SNSs for medical analysis issues. Afterward, the weighted cosine similarity measures of SNSs were used. Wang et al. [22] proposed a SVNS, which is the main example of NS for most applicable applications. Research of NS in medical diagnosis cover many problems are in different image modalities and different tasks such as denoising, clustering, classification.

3.1. Neutrosophic set in medical image denoising

Generally, the medical image consists of noises, these noises are kind of intermediate information. Removing noises from the medical images is an important research area in computer science. Dealing with indeterminacy in images under the NS theory helping in reaching better performance during the image preprocessing stage [43]. Many approaches rely on NS for reducing salt and pepper, speckle, rician, and gaussian noise are listed in Table 2.

In 2011 Mohan et al. [44] proposed a filter to remove noise from MRI image by converting it to NS domain. Then obtain the membership values of T, I, F. The γ-median filter used to decrease the indeterminacy entropy. This approach compared with the median filter and NLM filer and shows superior results. An extension for this study applies ω – wiener filter on MRI image [45]. Also, the same author expanded the study on nonlocal NS (NLNS) [46]. The results show superior result for ω – wiener with higher PSNR.

In 2012 Koundal et al. [47] applied Kuan filter and Lee filter on US image. An extension to this study [48] use Gamma variation on neutrosophic domain to improve image quality. The same author proposed a Nakagami distribution method based on NS. The results show superior results to Nakagami distribution approach based on NS.

Another contribution on RGB image in [49] aimed to improve the quality of image based on NSS. Another study on NSS in [50] on liver image. the results shows higher PSNR to [50] but [49] improve the contrast of image more better. Another contribution improved the NLM using the weighted function based on NL to enhance US image. Furthermore Ashour et al. [26] introduce a novel method for dermoscopic image denoising based on OIF which aims to optimize the

indeterminacy filter using GA. Also, Nasef et al. [51] improve the dark area in skeletal image based on NS and SSA under multi-criteria.

Table 2. Different medical image denoising methods using the NS theory.

Authors	Modality	Data	Noise	Gray /RGB	Denoising Method	Metric
Mohan et al. (2011) [44]	MRI	MRI brain (axial, Sagittal)	Rician	Gray	γ -median	PSNR* (Axial, Sagittal)= (19.90,19.11)
Mohan et al. (2012) [45]	MRI	Axial MRI brain	Rician	Gray	ω – wiener	SSIM†=0.9682 PSNR=24.08 QILV‡=0.9882
Koundal et al. (2012) [47]	US	Thyroid	Speckle	Gray	Kuan filter and Lee filter	SNR§ (Lee)=17.5375 SNR (Kuan) =17.0408 EPI¶ (Lee) = 0.7858 EPI (Kaun)=0.7599
Mohan et al. (2013) [46]	MRI	Axial MRI brain	Rician	Gray	nonlocal NS (NLNS) and ω – wiener	PSNR=23.92 SSIM= 0.9254
Koundal et al. (2016) [48]	US	Thyroid image	Synthetic Speckle	Gray	Based on gamma distribution	UQI‖ = 0.8606 FSIM#=0.8790 EPI = 0.8718 MSSIM**=0.8099 VIF& = 0.3565
Koundal et al.2018 [52]	US	Thyroid image	Synthetic Speckle	Gray	Based on Nakagami distribution	UQI = 0.8606 EPI = 0.8813 MSSIM=0.8139 VIF = 0.3771
Shahin et al. (2018a) [49]	MIA	blood smear images (3327 of different types of WBCs)	illumination, contrast, and color balance problems	RGB	Neutrosophic similarity score(NSS) scaling	Cost Time (Sec per image) from 0.276 s to 0.96 s
Rahimizadeh et al. (2019) [53]	US	Different organs	Speckle	Gray	Weighted function + (NLM) filter	SNR in noise level 0.4=53.36 SSIM for noise level 0.4=0.9514
Bharti et al.(2020) [50]	US	Liver	Speckle	Gray	(NSS)	PSNR= 34.18±1.80×10-1

						AMBE&&= 0.0326±9.87×10 -3 EPI= 0.9687±2.1×10- 3 UIQI^= 0.9757±1.17×10 -2 MS-SSIM^^= 0.9996±1.63×10 -4
Ashour et al. (2019)[26]	Dermoscop ic	20 randomly selected images (Internationa l Skin Imaging Collaboratio n)	synthetic Gaussian	Gray	Optimized indetermin acy filter (OIF) + genetic algorithm (GA)	SNR=27.75 PSNR=31.47 MSE++=57.86 RMSE°=7.18
Nasef et al. (2020) [51]	Skeletal scintigraph y	Data collected from Menoufia University Hospital in Egypt	Dark regions	Gray level	Salp Swarm algorithm (SSA) under multi- criteria	Results show that implementatio n achieves better performance in most criteria

*Key of Table 2***: *** Peak-signal-to-noise ratio, **†** Structural Similarity index, **‡** Quality Index based on local variance, **§** Signal-to-noise ratio, **¶** Edge preservation index, **||** Universal quality index, **#** Visual information fidelity, ****** Multi-scale structural similarity index metric , **&** Visual information fidelity , **&**Absolute mean brightness error , **^** universal image quality index , **^^** Multi-scale structural similarity, **++** Mean squared error , **°** The root of mean squared error

3.2. *Neutrosophic sets in medical image clustering and segmentation*

In computer vision Clustering means several grouped objects that are related in common members. On the other hand, segmentation in medical image separate object from the background so the image is separated into non-overlapping various regions. Clustering and segmentation are crucial processes in medical image diagnosis [23]. There are various approaches that use to segment and cluster the medical image using the NS theory in many medical applications as in Table 3.

Shahin et al. [54] proposed a new method for WBC segmentation using multi-scale similarity measure based on NS domain. This approach is obtained on RGB public dataset. Another proposed on RGB image, Ashour et al. [55] proposed a segmentation method on WBC image. This approach aims to detect blood cell by first using canny edge detector and then circular Hough transform (CHT) based on NS domain. Finally, K-means detect nuclei in blood cell image.

A study on dental image segmentation aimed to increase the accuracy in x-ray image by introducing a new fuzzy clustering methods based on NS orthogonal matrix [56]. Furthermore,

Ashour et al. [57] proposed an approach on dermoscopic grayscale image based on clustering histogram. The histogram clustering method aims to determine the needed number of clusters in NS c-means.

On breast cancer segmentation, Lotfollahi et al. [58] proposed a new method based on active contour to detect the tumor outline. Then the initial contour is defined depending on intensity and NS feature. Another study on breast cancer CT image, by first transform the CT image to NS domain. Then apply RGI segmentation algorithm for lesion segmentation [59]. Guo et al. [60] introduced an approach for Skin lesion segmentation based on NCM and KGC. This approach shows superior result than using KGC only or traditional GC.

In brain tumor segmentation Palanisamy et al. [61] introduced the integration between NS and FCM and optimizing the clustering using modified PSO. Another contribution on brain tumor segmentation, by Singh [62] proposed a T2NS method for selecting multi adaptive threshold to segment brain lesions. This approach shows superior results on neutrosophic-based adaptive threshold. Also, Tufail et al. [63] proposed a method to extract ROI under NS domain based on modified s-function.

In Parkinson's disease, Singh [64] proposed methods based on neutrosophic based adaptive threshold for segmentation. This approach aimed to solve two problems, first is the gray and white boundaries, second unclear gray regions. An expand for this work, which composed of two parts NEBCA for segmentation and HSV color system for better representation.

Table 3. Different medical image segmentation/clustering methods using the NS theory.

Authors	Modality	Organ	Gray/RGB	Methods	Evaluation metric
Shahin et al. (2018b) [54]	MIA	WBC	RGB	multi-scale similarity measure	Precision= 97.2%
Ali et al. (2018) [56]	x-ray	Dental	Gray level	NS orthogonal principle	Davies-Bouldin =10.562 Simplified silhouete width criterion (SSWC)=0.941 Visibility metric (VM)=484.002
Ashour et al. (2018) [57]	Dermoscopic	skin lesion	Gray level	Histogram-based clustering estimation (HBCE) and neutrosophic c-means (NCM)	Accuracy= 96.3%
Lotfollahi et al. (2018) [58]	US	Breast	Gray level	Active contour models	True positives (TP)=95% False positives (FP)=6% Similarity scores=90%

. Lee et al. (2018) [59]	CT	Breast lesion	Gray level	RGI integrated with NS	Dice coefficient (DC) =0.82 AUC = 0.8
Guo et al. (2019) [60]	Dermoscopic images	Skin lesion segmentation	Gray level	(NCM) and kernel graph cut(KGC)	Accuracy= 97.41% DC = 93.27% Jaccard similarity coefficients (JAC) = 87.78% Sensitivity=99.21%
Ashour et al. (2019) [55]	MIA	WBC	RGB	Canny detector, circular Hough transform (CHT) and k-means	Accuracy=98.44% DC=93.10% JAC= 87.14% Sensitivity=95.08%
Palanisamy et al. (2019) [61]	MRI	Brain tumor	Gray level	Fuzzy C-mean (FCM) clustering guided with a modified particle swarm optimization (PSO)	Sensitivity=95.43% Specificity=98.58% JAC= 87.56% DC= 94.32%
Singh (2020) [64]	MRI	Parkinson's disease	Gray level	Adaptive threshold and neutrosophic entropy based	Result for testing data PSNR=62.99 MSE= 0.10 SSIM= 0.7006
Singh (2020) [65]	MRI	Parkinson's disease	Gray level	neutrosophic-entropy based clustering algorithm (NEBCA), and HSV color system.	**(Result of HSV color system based on testing set)** standard deviation (SD)= 13885000 total neutrosophic entropy information (TNEI) =323670
Singh (2021) [62]	MRI	Brain tumors	Gray level	Type-2 NS (T2NS) entropy and multiple threshold	**Result of sets (Set I, Set II and Set III)** JAC=97.07%, 97.92% ,97.13% Correlation coefficients=0.9638, 0.9698 ,0.9610 Uniformity measures = 0.9624, 0.9633 and 0.9660

Tufail et al. (2021) [63]	MRI	Detect ROI Brain tumor	Gray level	ROI in tumor images extract using S-function	Sensitivity=98%, false negative (FN) =1.5%

3.3. Neutrosophic sets in medical image classification

NS classification is achieving success because of its use of simple procedures. The NS classifier utilizes NL to manage the gain noise and indeterminacy. We summarized all studies in Table 4.

Xian et al.[66] introduced neutrosophic subset and neutrosophic connectedness. This approach showed it's results on breast US images with superior performance than fuzzy connectedness. Moreover, Gaber et al.[67] proposed a segmentation and classification approach for thermogram image. in segmentation, an integration between NS and FCM was introduced. In classification, a SVM is used to normal or abnormal regions. Another study proposed a SVM as classifier by combining texture and morphological features.

Table 4. Different medical image classification methods using the NS theory.

Author	Year	Modality	Task	Method using NS
Xian et al.[66]	(2014)	US	Breast	Neutro-Connectedness
Gaber et al.[67]	(2015)	Thermogram	Breast	Fast fuzzy c-means (FFCM)
Amin et al. [68]	(2016)	US	Breast	NS score

4. Deep learning in medical image analysis

DL has great success over traditional ML algorithms. Neural networks (NN) are the key foundation for DL. It is implemented with more than two layers to permit non-linear operations, Which makes it widely used in medical image Denoising and clustering, segmentation, and classification phases [23].

Learning strategies are divided into supervised, semi-supervised, and unsupervised algorithms. SL has a labeled data that intends to learn the function of given data, Semi-supervised learning (SSL) intends to learn unlabeled data points using knowledge learned from labeled data. Unsupervised learning (USL) has not any label data, so its objective is to deduce the real structure present with a group of the data point.

At Present, CNN and RNN are widely utilized in medical image diagnosis as (SL). On the other hand, the Auto-encoder (AE), Restricted boltzmann machine (RBM), and DBN are widely used as (USL)or (SSL). In the following Table 5. there is a brief on Different DL architectures [23]. Koundal et al.2018 [52].

Table 5. Different DL architecture in SL, SSL, and USL

SL			
Architecture	**Variants**	**Main feature**	**Main problem**
CNN	LeNet Alexnet VGGnet Resnet GoogleNet	-parameter sharing -spatial relationship	Require labeled data and large scale of data
RNN	LSTM	-parameter sharing -recurrent connections	-Vanishing /exploding gradient problem
USL or SSL			
Architecture	**Main features**		**Main problem**
AE	-Has unidirectional connection - Greedy strategy is implemented in each layer		Require a pretrained phase
RBM	More general than DBN where all edges are indirect		Cannot Optimizing parameters during large scale of data
DBN	Is probabilistic generative model with an RBM.		High computation Training process results from initialization

4.1. DL in medical image denoising

One of famous medical noisy image is additive white noisy images which can be salt and pepper, gaussian, and poison noisy images. Also, real noisy image is considered one of denoising problem as it comprises blurry and false image artifacts.in the other hand, there is a need for DL technique to overcome the real complex and noise which results from image corruption. Sometimes the images consist of hybrid types of noises [69].Some of DL techniques to solve noisy image problem follows in Table 6.

Table 6. DL techniques in medical image denoising.

Ref.	Method	Modalities	Noise
Ma et al. (2018) [70]	conditional Generative adversarial network (cGAN)	Retinal OCT	Speckle (Edge preservation)
Meng et al.(2020)[71]	CNN	CT	Low-dose CT imaging
Chai et al.(2019)[72]	hierarchical deep generative adversarial networks (HD-GANs)	CT	Low-dose CT imaging
Jifara et al. (2019)[73]	CNN using residual learning	x-ray	Poison

| Gholizadeh-Ansari et al.(2018)[74] | CNN using residual learning | CT, x-ray | Low dose |

4.2. *Deep learning in medical image clustering and segmentation*

Lesions and organs segmentation is an important area in DL. Some semantic segmentation research works have been done over various segmentation modalities and organs are shown in Table 7.

Table 7. DL techniques in medical segmentation.

Authors	Modality	Organ	Methods
Konstantinos et al. (2017) [75]	MRI	brain	3D FCNN, CRF
Zilly et al. (2017) [76]	Retinal image	Glaucoma	Simple CNN, sequential learned to use boosting.
Abdel-Basset et al. (2021) [77]	CT	Covid-19	Implement FSS-2019-nCov architecture based on Few-shot learning (MSLPNet)
Chen et al. (2021) [78]	X-ray	Dental	multi-scale location perception network
Ding et al. (2021) [79]	MRI	Brain	Informed DL segmentation (FI-DL-Seg) network

4.3. *Deep learning in medical image classification*

DL shows precedence success in image classification. CNN is the most used architecture since the propositions of Alexnet 2012 by [8]. Which becomes the beginning of many architectures depending on CNN such as GoogleNet, VGG, and Resnet. Many studies show its effort in DL in medical image classification shows in Table 8.

Table 8. DL techniques in medical image classification.

Author	Year	Modality	Task	Method
Pinaya et al. [80]	2016	Brain morphography	Schizophrenia	DBN
Fu et al. [81]	2018	Retinal	Glaucoma	M-Net
Zhang et al.[82]	2019	Different modalities	Multi-classification task	Multiple DCNNs
Wang et al. [83]	2020	CT	Liver	CNN

5. Deep learning in medical image analysis using NS theory

Some studies show results of NS integration with DL algorithms in medical images analysis with explores in this section and in the following Table 9.

Table 9: Summarization of different studies in medical image analysis using NS-based DL models.

Author	Organ/modality	Task	DL architecture
Guo et al. (2019) [84]	Skin lesion	classification	DCNN
Özyurt et al.(2019) [85]	Brain tumor	Segmentation, classification	CNN with neutrosophic expert maximum fuzzy (NS-CNN) sure entropy
Khalifa et al. (2020) [86]	X-ray Covid-19	Classification	Alexnet, GoogleNet, Resnet
Cai et al. (2019) [87]	mammogram Breast cancer	Classification	DCNN
Shain et al. (2020) [88]	cardio location	Classification	CNN architectures, LSTM

MDCNN is proposed by Guo et al.(2019) [84] for skin dermoscopic image classification between melanoma(malignant) and nevi(benign). First, Guo et al. implement DCNN architecture consists of convolution, ReLU (rectified linear unit), pooling, softmax, and classification layer. For speeding up the training phase, multiple pre-trained CNN models were applied with transfer learning (TL), where a neutrosophic reinforcement sample learning (NRSL) strategy is introduced in the MDCNN. Usually, the NRSL is not used in a single DCNN training; the NRSL is used in the model to develop the next DCNN samples in the MDCNN model.

The ISIC2016 dataset was joined to assess the proposed NMDCNN model as in Figure 1. For every DCNN, the implemented NRSL TL-based was introduced to train each DCNN model on the different samples. The NSS was introduced to define the reinforced training time, which differs based on sample performance. This procedure was replicated for every DCNN in the MDCNN, selection criteria based on the previous model previous score.

An MDCNN architecture is constructed by follow multiple networks of the same implementation. For Q, the total number of DCNNs samples, the MDCNN can be expressed as:

$$MDCNN = \{CNN_1, CNN_2, \ldots, CNN_q\}$$

Normally, every DCNN, usual training was used while the incremental learning was used to generate samples for the next DCNN as follows:

$$SP_{q+1} = \{SP_q, ReInSP_q\}$$

where SP_q and SP_{q+1} are the sample for the qth DCNN and (q+1)th DCNN, respectively, and $ReInSP_q$ is the reinforcement sample for the (q+1)th DCNN.

The voting scheme is used for evaluating the classification results. The results show the effect of the NMDCNN model on testing, training accuracies with 97.78%, 85.22% respectively.

| (**a**) | (b) |
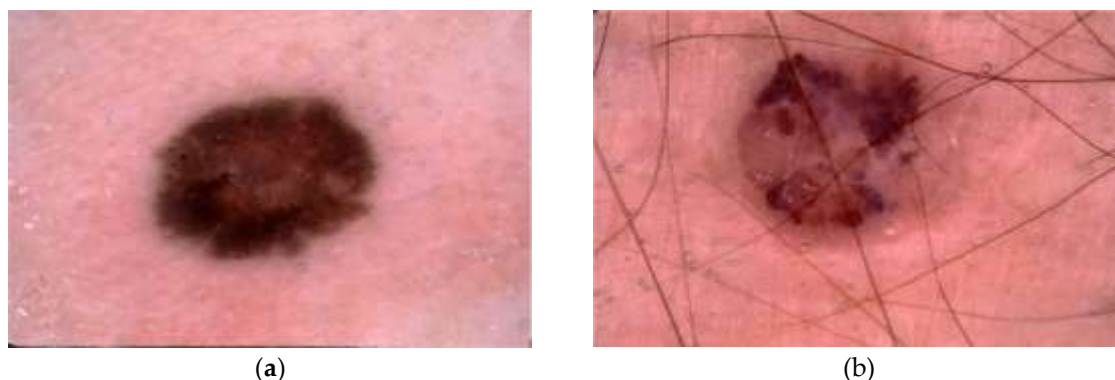
Figure 1. Samples from demoscopic dataset: (A) benign (nevus) (B) malignant.

Cai et al. [87] introduced an NS-DL technique to detect breast cancer in the mammogram. The proposed consists of five stages as in Figure 2. The test is done using data gathered from Nanfang Hospital (NFH), Guangzhou, China, and the publicly available [89].

In the coarse stage detection, the thresholding method is used for image binarization, and the connected component analysis classifies the binary image regions to (TP) and (FP). The DCNN1 is the training phase based on DCNN architecture. In Traditional DCNN, all samples are trained in fixed time so, adding NRSL strategy through the training phase trains samples in adaptive time.

The Microcalcifications (MC) clustering phase done using density-based spatial clustering of applications with a noise (DBSCAN) algorithm which has high adaptability with noise. The second classifier (DCNN2) is used to train the data set while DCNN1 is only for MC detection and FP deduction.

The final stage is diagnosis and testing for data to give the probability of malignancy using a bounding box. The results of MC detection stage 92% sensitivity and0.50 FP per image in cluster evaluation. After 40 epochs, training, validation, and testing accuracies are 99.87%, 95.12%, and 93.68% respectively while, 98.03%, 93.49%, and 92.36% for comparative. Methods AUC for validation and testing 0.908 and 0.872 for DCNN2.
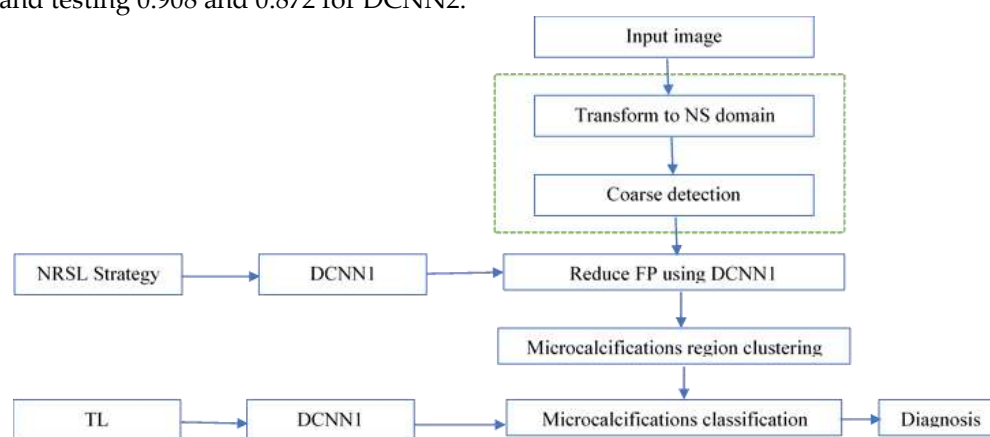
Figure 2. Breast cancer detection architecture based on NS and DL.

Özyurt et al.(2019) [85] classified the segmented brain tumor using hybridization between NS and CNN(NS-CNN). To test the proposed approach The Cancer Genome Atlas Glioblastoma Multiforme (TCGA-GBM) data collection in The Cancer Imaging Archive (TCIA) was used. The proposed (NS-EMFSE-CNN) is consists of 3 stages: segmentation, feature extraction, and classification as in Figure 3.

The first stage segments the MRI brain using the NS-EMFSE algorithm. This algorithm consists of three steps. In the first step, some pre-processing techniques are applied to (T1-GD sequence) MR. In the second step the NS- EMFSE method transform the filtered image NS image then converts it to a binary image. The last step is cleaning residual pixels and fill gaps in the edge image. This process is reviewed in Algorithm 1.

| **Algorithm 1: Image Segmentation using NS-EMFSE**	
1.Getting brain MRI from dataset.	
2. Convert the image to grayscale form.	Step 1
3.Apply adaptive winner filter to gray scale image.	
4.Using NS-EMFSE method to convert filtered image into binary image.	Step 2
5.Cleannig residual pixels in binary image.	Step 3
6.Filling gaps.	
The finally segmented image is obtained in algorithm 2 for training and testing preparation	

Algorithm 2: Image preparation for training and testing
1. Get the corresponding white colored points in the segmented image.
2. Get the corresponding points in the original image.

The second stage in NS-EMFSE-CNN is feature extraction which is done using Alexnet architecture based on CNN to avoid manual feature extraction. The fully connected layer (FC7) in Alextnet obtain 4096 features which are given to the next stage of classification as in Figure 3.

The final stage is a classification which is done using Support vector machine (SVM) and K-nearest neighbor (KNN) classifiers. The results show higher accuracy when using SVM classifier than KNN. Also shows high sensitivity for both classifiers which indicates that feature is more judicial to benign tumors. At the same time, specificity rates were lower which indicates that malignant tumor features were less notable.
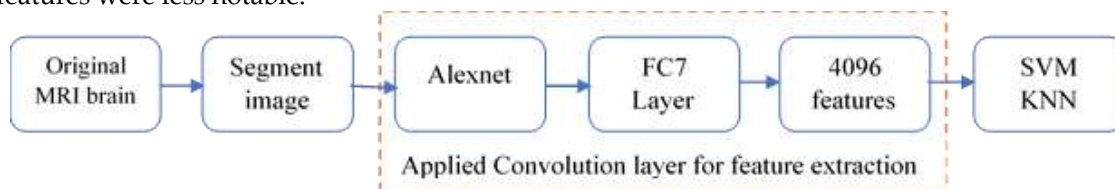
Figure 3. (NS-EMFSE-CNN) architecture

Khalifa et al. [86] provided a study that shows the effect of hybrid NS and DTL on classification. The study work on Covid-19 x-ray dataset images. It was gathered from various websites such as the Italian Society of Medical, online publications, and the Radiopaedia web. The formed dataset is arranged into four categories normal, pneumonia bacterial, pneumonia virus, and COVID-19 with several images 79, 79, and 79, and 69, respectively.

The NS-DTL model first converted the original image to the NS image So every pixel in the image has been divided into three subsets (T, I, F). Then applied different DTL model with DL strategies under specific hyperparameter for training and testing phases such as in Table 10. More than 36 trails had been conducting to assess the performance of the NS conversion. Four domains of images are tested, and they are the original images T, I, and F images such as in Figure 4.
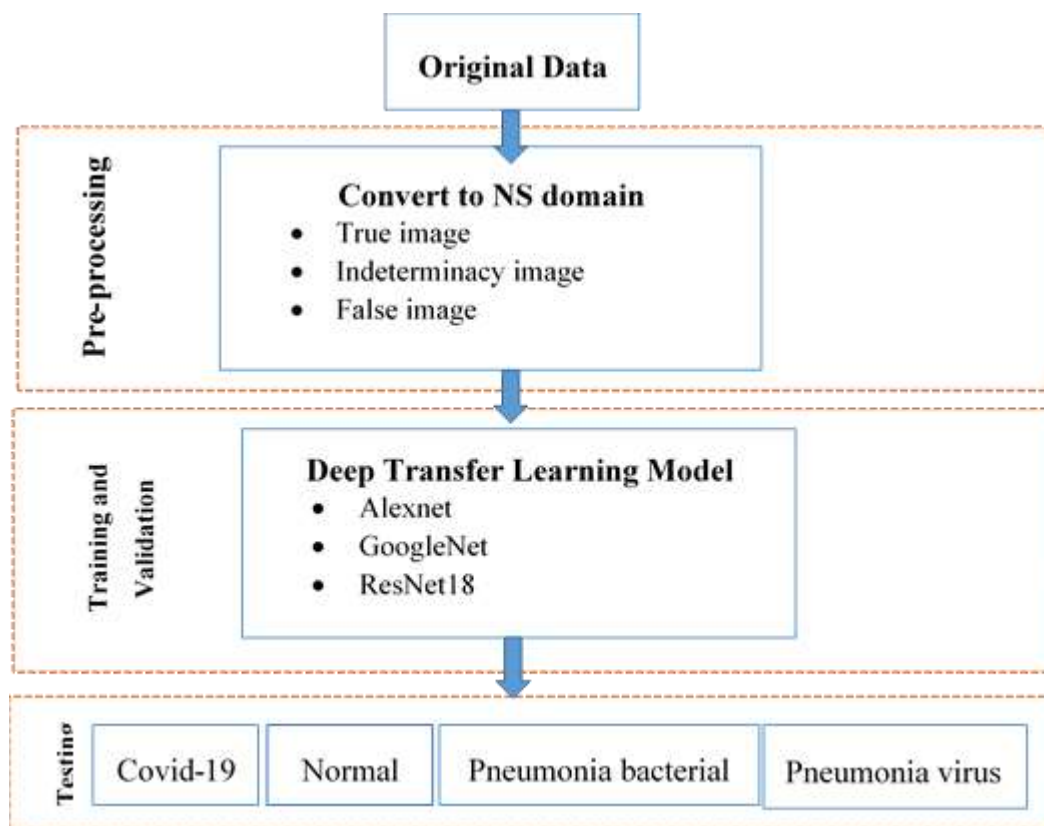
Figure 4. NS/DTL model

Table 10. Ns-DTL learning strategies, models and hyperparameters.

Different training and testing strategies
Training-Testing
70% – 30%.
80% – 20%.
90% – 10%.
Different DT models
Resnet18
Googlenet
Alexnet
Hyperparameters
Optimizer: Adaboost
Momentum: 0.9
Epochs: 50
Early stopping: 10 epochs
Batch size: 32
Learning Rate: 0.001

According to the experimental results, the maximum accuracy possible in the testing accuracy and performance metrics such as F1Score, recall, precision was achieved by the Indeterminacy (I) NS domain.

Shain et al. [88] proposed a classification framework to classify the 3-location of cardio view. The proposed integrated the LSTM and CNN architecture as in Figure 5. Also, the proposed use of NS to extract the temporal descriptor to combine the spatial and NS temporal. Then Using CNN as a pre-trained model. Lastly, utilize LSTM to classify each echo clip into eight cardio-views.
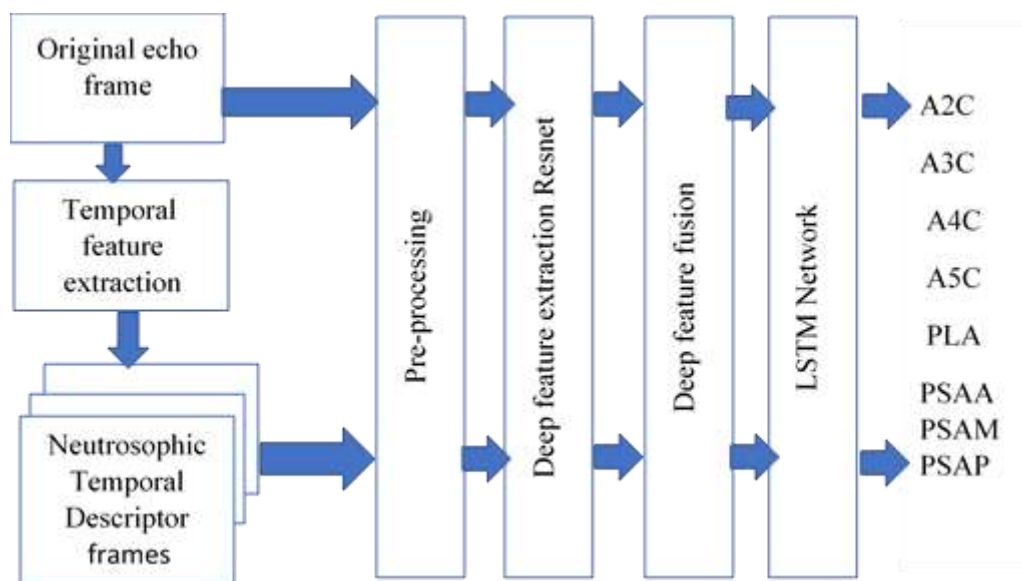
Figure 5. Eight cardio-views classification system.

Echocardiography clips consist of frames each frame has a spatial descriptor, which is converted to a temporal descriptor using the NS theory. Then a preprocessing stage of resizing spatial and temporal frames to fit the pre-trained network.

The proposed use of both spatial and temporal descriptors for CNN feature extraction. The feature extraction phase is done using CNN architectures such as Alexnet, VGGNets, GoogleNet, Densenet, and ResNets. The next stage is feature fusion which gathers the latest information of cascading spatial and temporal descriptors from FC layers of both model's streams. Finally, LSTM is used to classify the fused CNN features. LSTM the implementation is done using Quad-Core 2.9 GHz Intel i5 with 16 GB of memory, and moderate graphic processing unit NVIDIA TITAN-Xp GPU with 12 GB RAM.

The results show that ResNet101 achieves the highest performance in Spatial-temporal and fusion features with an accuracy score of 96.3% and 99.1% for cardio location classification.

6. Conclusion and future works

Recent progress in the deep learning research area shows a successful impact on medical image analysis. Deep learning performance can be improved via integration with neutrosophic systems. Recently, deep learning performance was affected by noise, ambiguity, or incomplete data, which are the major problems in medical data images.

At the time being, many researchers aim to tackle these issues by using neutrosophic systems. Some studies show that the hybridization of neutrosophic theory and deep learning can enhance the performance of medical image analysis where data are noisy, fuzzy, incomplete, or ambiguous. Neutrosophic systems can be used as an essential part of deep learning models by using neutrosophic reinforcement sample learning to speed up the training procedure and reinforce training to the poor performance samples with more times according to their performance. Neutrosophic image transformation (T, I, F) for each pixel can increase the computational complexity, but it provides great resistance to noise. The availability of software platforms such as Intel MKL, AMD ROCm, and Nvidia CUDA can speed up deep learning processes.

In almost all neutrosophic sets in medical image analysis or in hybridization between Neutrosophic sets and deep learning, image conversion to the neutrosophic image has been carried using the same equations, which used in all medical image modalities, all different stages in image analysis, and with any deep learning architecture integration. Every case in medical image analysis requires convenient define of membership function.

At present, some research efforts show the results of deep learning and neutrosophic set integration. But there is an essential need to show studies in neutrosophic in deep learning parameter optimizing, neutrosophic with medical big data analysis, and various types of medical image modalities and applications. So, more comprehensive studies should be developed, such as studies on fuzzy neural networks. Enhancing the performance of neutrosophic deep learning models can be explored in the future.

References

[1]   H. Brody, "Medical imaging," *Nature,* vol. 502, pp. S81-S81, 2013.

[2]   D. Shen, G. Wu, and H.-I. Suk, "Deep learning in medical image analysis," *Annual review of biomedical engineering,* vol. 19, pp. 221-248, 2017.

[3]   J. Haugeland, *Artificial intelligence: The very idea*: MIT press, 1989.

[4]   G. Litjens, T. Kooi, B. E. Bejnordi, A. A. A. Setio, F. Ciompi, M. Ghafoorian, *et al.*, "A survey on deep learning in medical image analysis," *Medical image analysis,* vol. 42, pp. 60-88, 2017.

[5]   F. Altaf, S. M. Islam, N. Akhtar, and N. K. Janjua, "Going deep in medical image analysis: concepts, methods, challenges, and future directions," *IEEE Access,* vol. 7, pp. 99540-99572, 2019.

[6]   I. Goodfellow, Y. Bengio, A. Courville, and Y. Bengio, *Deep learning* vol. 1: MIT press Cambridge, 2016.

[7]   Y. LeCun, L. Bottou, Y. Bengio, and P. Haffner, "Gradient-based learning applied to document recognition," *Proceedings of the IEEE,* vol. 86, pp. 2278-2324, 1998.

[8]   A. Krizhevsky, I. Sutskever, and G. E. Hinton, "Imagenet classification with deep convolutional neural networks," *Advances in neural information processing systems,* vol. 25, pp. 1097-1105, 2012.

[9]   J. L. McClelland, D. E. Rumelhart, and P. R. Group, *Parallel distributed processing* vol. 2: MIT press Cambridge, MA, 1986.

[10]   K. Mondal, P. Dutta, and S. Bhattacharyya, "Fuzzy logic based gray image extraction and segmentation," *International Journal of Scientific & Engineering Research,* vol. 3, pp. 1-14, 2012.

[11]   A. Q. Ansari, R. Biswas, and S. Aggarwal, "Proposal for applicability of neutrosophic set theory in medical AI," *International Journal of Computer Applications,* vol. 27, pp. 5-11, 2011.

[12]   G. Deschrijver and E. E. Kerre, "On the relationship between some extensions of fuzzy set theory," *Fuzzy sets and systems,* vol. 133, pp. 227-235, 2003.

[13]   H. J. Zimmermann, "Fuzzy set theory," *Wiley Interdisciplinary Reviews: Computational Statistics,* vol. 2, pp. 317-332, 2010.

[14]   W. Feller, *An introduction to probability theory and its applications, vol 2*: John Wiley & Sons, 2008.

[15]   Y. Yang, C. Zheng, and P. Lin, "Fuzzy C-means clustering algorithm with a novel penalty term for image segmentation," *Optoelectronics Review,* vol. 13, p. 309, 2005.

[16]   F. Smarandache, S. Broumi, P. K. Singh, C.-f. Liu, V. V. Rao, H.-L. Yang, *et al.*, "Introduction to neutrosophy and neutrosophic environment," in *Neutrosophic Set in Medical Image Analysis*, ed: Elsevier, 2019, pp. 3-29.

[17]   F. Smarandache and N. P. Neutrosophy, "Set, and Logic, ProQuest Information & Learning," *Ann Arbor, Michigan, USA,* p. 105, 1998.

[18]   R. Kala, R. Janghel, R. Tiwari, and A. Shukla, "Diagnosis of breast cancer by modular evolutionary neural networks," *International Journal of Biomedical Engineering and Technology,* vol. 7, pp. 194-211, 2011.

[19]   K. C. Tan, Q. Yu, C. Heng, and T. H. Lee, "Evolutionary computing for knowledge discovery in medical diagnosis," *Artificial Intelligence in Medicine,* vol. 27, pp. 129-154, 2003.

[20]   S. A. Hussain and M. P. Raju, "Neuro-fuzzy system for medical image processing," in *2010 International Conference on Communication and Computational Intelligence (INCOCCI),* 2010, pp. 382-385.

[21]   J. Ye, "Improved cosine similarity measures of simplified neutrosophic sets for medical diagnoses," *Artificial intelligence in medicine,* vol. 63, pp. 171-179, 2015.

[22]   G. Priest, "Paraconsistent logic," in *Handbook of philosophical logic*, ed: Springer, 2002, pp. 287-393.

[23]   G. N. Nguyen, A. S. Ashour, and N. Dey, "A survey of the state-of-the-arts on neutrosophic sets in biomedical diagnoses," *International Journal of Machine Learning and Cybernetics,* vol. 10, pp. 1-13, 2019.

[24]   A. Sengur, U. Budak, Y. Akbulut, M. Karabatak, and E. Tanyildizi, "A survey on neutrosophic medical image segmentation," in *Neutrosophic Set in Medical Image Analysis*, ed: Elsevier, 2019, pp. 145-165.

[25]   X. Peng and J. Dai, "A bibliometric analysis of neutrosophic set: Two decades review from 1998 to 2017," *Artificial Intelligence Review,* vol. 53, pp. 199-255, 2020.

[26]   A. S. Ashour and Y. Guo, "Advanced optimization-based neutrosophic sets for medical image denoising," in *Neutrosophic set in medical image analysis*, ed: Elsevier, 2019, pp. 101-121.

[27]   D. Koundal and B. Sharma, "Challenges and future directions in neutrosophic set-based medical image analysis," in *Neutrosophic Set in Medical Image Analysis*, ed: Elsevier, 2019, pp. 313-343.

[28]   D. Koundal and B. Sharma, "Advanced neutrosophic set-based ultrasound image analysis," in *Neutrosophic set in medical image analysis*, ed: Elsevier, 2019, pp. 51-73.

[29]   A. Shahin, Y. Guo, and A. S. Ashour, "Advanced neutrosophic sets in microscopic image analysis," in *Neutrosophic Set in Medical Image Analysis*, ed: Elsevier, 2019, pp. 31-50.

[30]   A. Elhassouny, S. Idbrahim, and F. Smarandache, *Machine learning in Neutrosophic Environment: A Survey*: Infinite Study, 2019.

[31]   M. I. Razzak, S. Naz, and A. Zaib, "Deep learning for medical image processing: Overview, challenges and the future," *Classification in BioApps,* pp. 323-350, 2018.

[32]   J. Ker, L. Wang, J. Rao, and T. Lim, "Deep learning applications in medical image analysis," *Ieee Access,* vol. 6, pp. 9375-9389, 2017.

[33]   O. Faragallah, H. El-Hoseny, W. El-Shafai, W. Abd El-Rahman, H. S. El-Sayed, E.-S. El-Rabaie, *et al.*, "A Comprehensive Survey Analysis for Present Solutions of Medical Image Fusion and Future Directions," *IEEE Access,* 2020.

[34]   P. Gravel, G. Beaudoin, and J. A. De Guise, "A method for modeling noise in medical images," *IEEE Transactions on medical imaging,* vol. 23, pp. 1221-1232, 2004.

[35]   S. Senthilraja, P. Suresh, and M. Suganthi, "Noise reduction in computed tomography image using WB filter," *International Journal of Scientific and Engineering Research,* vol. 5, pp. 243-247, 2014.

[36]   D. C. Wilbur, K. Madi, R. B. Colvin, L. M. Duncan, W. C. Faquin, J. A. Ferry, *et al.*, "Whole-slide imaging digital pathology as a platform for teleconsultation: a pilot study using paired subspecialist correlations," *Archives of pathology & laboratory medicine,* vol. 133, pp. 1949-1953, 2009.

[37]   F. Smarandache, *A unifying field in logics: neutrosophic logic. Neutrosophy, neutrosophic set, neutrosophic probability: neutrsophic logic. Neutrosophy, neutrosophic set, neutrosophic probability*: Infinite Study, 2005.

[38]   M. Zhang, L. Zhang, and H.-D. Cheng, "Segmentation of ultrasound breast images based on a neutrosophic method," *Optical Engineering,* vol. 49, p. 117001, 2010.

[39]   D. KOUNDAL, S. GUPTA, and S. SINGH, *Applications of Neutrosophic Sets in Medical Image Denoising and Segmentation*: Infinite Study.

[40]   Y. Guo and H.-D. Cheng, "New neutrosophic approach to image segmentation," *Pattern Recognition,* vol. 42, pp. 587-595, 2009.

[41]   L. Zhang and Y. Zhang, "A novel region merge algorithm based on neutrosophic logic," *International Journal of Digital Content Technology and its Applications,* vol. 5, pp. 381-7, 2011.

[42]   Y. Guo, H. Cheng, and Y. Zhang, "A new neutrosophic approach to image denoising," *New Mathematics and Natural Computation,* vol. 5, pp. 653-662, 2009.

[43]   P. Arulpandy, *Reduction of indeterminacy of gray-scale image in bipolar neutrosophic domain*: Infinite Study, 2019.

[44]   J. Mohan, V. Krishnaveni, and Y. Guo, "A neutrosophic approach of MRI denoising," in *2011 International Conference on Image Information Processing*, 2011, pp. 1-6.

[45]   J. Mohan, Y. Guo, V. Krishnaveni, and K. Jeganathan, "MRI denoising based on neutrosophic wiener filtering," in *2012 IEEE International Conference on Imaging Systems and Techniques Proceedings*, 2012, pp. 327-331.

[46]   J. Mohan, V. Krishnaveni, and Y. Guo, "MRI denoising using nonlocal neutrosophic set approach of Wiener filtering," *Biomedical Signal Processing and Control,* vol. 8, pp. 779-791, 2013.

[47]   D. Koundal, S. Gupta, and S. Singh, "Speckle reduction filter in neutrosophic domain," in *Int. Conf. of Biomedical Engineering and Assisted Technologies*, 2012, pp. 786-790.

[48]   D. Koundal, S. Gupta, and S. Singh, "Speckle reduction method for thyroid ultrasound images in neutrosophic domain," *IET Image Processing,* vol. 10, pp. 167-175, 2016.

[49]   A. Shahin, K. Amin, A. A. Sharawi, and Y. Guo, "A novel enhancement technique for pathological microscopic image using neutrosophic similarity score scaling," *Optik,* vol. 161, pp. 84-97, 2018.

[50]   P. Bharti and D. Mittal, "An Ultrasound Image Enhancement Method Using Neutrosophic Similarity Score," *Ultrasonic Imaging,* vol. 42, pp. 271-283, 2020.

[51]   M. M. Nasef, F. T. Eid, and A. M. Sauber, "Skeletal scintigraphy image enhancement based neutrosophic sets and salp swarm algorithm," *Artificial Intelligence in Medicine,* vol. 109, p. 101953, 2020.

[52]   D. Koundal, S. Gupta, and S. Singh, "Neutrosophic based Nakagami total variation method for speckle suppression in thyroid ultrasound images," *IRBM,* vol. 39, pp. 43-53, 2018.

[53]   N. Rahimizadeh, R. P. Hasanzadeh, M. Ghahramani, and F. Janabi-Sharifi, "A Neutrosophic based Non-Local Means Filter for Despeckling of Medical Ultrasound Images," in *2019 9th International Conference on Computer and Knowledge Engineering (ICCKE)*, 2019, pp. 249-254.

[54]   A. I. Shahin, Y. Guo, K. M. Amin, and A. A. Sharawi, "A novel white blood cells segmentation algorithm based on adaptive neutrosophic similarity score," *Health information science and systems,* vol. 6, p. 1, 2018.

[55]   A. S. Ashour, Y. Guo, and A. R. Hawas, "Neutrosophic hough transform for blood cells nuclei detection," in *Neutrosophic Set in Medical Image Analysis*, ed: Elsevier, 2019, pp. 207-227.

[56]   M. Ali, M. Khan, and N. T. Tung, "Segmentation of dental X-ray images in medical imaging using neutrosophic orthogonal matrices," *Expert Systems with Applications,* vol. 91, pp. 434-441, 2018.

[57]   A. S. Ashour, Y. Guo, E. Kucukkulahli, P. Erdogmus, and K. Polat, "A hybrid dermoscopy images segmentation approach based on neutrosophic clustering and histogram estimation," *Applied Soft Computing,* vol. 69, pp. 426-434, 2018.

[58]   M. Lotfollahi, M. Gity, J. Y. Ye, and A. M. Far, "Segmentation of breast ultrasound images based on active contours using neutrosophic theory," *Journal of Medical Ultrasonics,* vol. 45, pp. 205-212, 2018.

[59]   J. Lee, R. M. Nishikawa, I. Reiser, and J. M. Boone, "Neutrosophic segmentation of breast lesions for dedicated breast computed tomography," *Journal of Medical Imaging,* vol. 5, p. 014505, 2018.

[60]   Y. Guo and A. S. Ashour, "Neutrosophic sets in dermoscopic medical image segmentation," in *Neutrosophic Set in Medical Image Analysis*, ed: Elsevier, 2019, pp. 229-243.

[61]   T. S. C. A. Palanisamy, M. Jayaraman, K. Vellingiri, and Y. Guo, "Optimization-based neutrosophic set for medical image processing," in *Neutrosophic Set in Medical Image Analysis*, ed: Elsevier, 2019, pp. 189-206.

[62]   P. Singh, "A type-2 neutrosophic-entropy-fusion based multiple thresholding method for the brain tumor tissue structures segmentation," *Applied Soft Computing,* vol. 103, p. 107119, 2021.

[63]   Z. Tufail, A. R. Shahid, B. Raza, T. Akram, and U. I. Janjua, "Extraction of region of interest from brain MRI by converting images into neutrosophic domain using the modified S-function," *Journal of Medical Imaging,* vol. 8, p. 014003, 2021.

[64]   P. Singh, "A neutrosophic-entropy based adaptive thresholding segmentation algorithm: A special application in MR images of Parkinson's disease," *Artificial Intelligence in Medicine,* vol. 104, p. 101838, 2020.

[65]   P. Singh, "A neutrosophic-entropy based clustering algorithm (NEBCA) with HSV color system: A special application in segmentation of Parkinson's disease (PD) MR images," *Computer methods and programs in biomedicine,* vol. 189, p. 105317, 2020.

[66]   M. Xian, H.-D. Cheng, and Y. Zhang, "A fully automatic breast ultrasound image segmentation approach based on neutro-connectedness," in *2014 22nd International Conference on Pattern Recognition*, 2014, pp. 2495-2500.

[67]   T. Gaber, G. Ismail, A. Anter, M. Soliman, M. Ali, N. Semary, *et al.*, "Thermogram breast cancer prediction approach based on Neutrosophic sets and fuzzy c-means algorithm," in *2015 37th Annual International Conference of the IEEE Engineering in Medicine and Biology Society (EMBC)*, 2015, pp. 4254-4257.

[68]   K. M. Amin, A. Shahin, and Y. Guo, "A novel breast tumor classification algorithm using neutrosophic score features," *Measurement,* vol. 81, pp. 210-220, 2016.

[69]   C. Tian, L. Fei, W. Zheng, Y. Xu, W. Zuo, and C.-W. Lin, "Deep learning on image denoising: An overview," *Neural Networks,* 2020.

[70]   Y. Ma, X. Chen, W. Zhu, X. Cheng, D. Xiang, and F. Shi, "Speckle noise reduction in optical coherence tomography images based on edge-sensitive cGAN," *Biomedical optics express,* vol. 9, pp. 5129-5146, 2018.

[71]   M. Meng, S. Li, L. Yao, D. Li, M. Zhu, Q. Gao, *et al.*, "Semi-supervised learned sinogram restoration network for low-dose CT image reconstruction," in *Medical Imaging 2020: Physics of Medical Imaging*, 2020, p. 113120B.

[72] K. Choi, M. Vania, and S. Kim, "Semi-supervised learning for low-dose ct image restoration with hierarchical deep generative adversarial network (hd-gan)," in *2019 41st Annual International Conference of the IEEE Engineering in Medicine and Biology Society (EMBC)*, 2019, pp. 2683-2686.

[73] W. Jifara, F. Jiang, S. Rho, M. Cheng, and S. Liu, "Medical image denoising using convolutional neural network: a residual learning approach," *The Journal of Supercomputing,* vol. 75, pp. 704-718, 2019.

[74] M. Gholizadeh-Ansari, J. Alirezaie, and P. Babyn, "Low-dose CT denoising with dilated residual network," in *2018 40th Annual International Conference of the IEEE Engineering in Medicine and Biology Society (EMBC)*, 2018, pp. 5117-5120.

[75] K. Kamnitsas, C. Ledig, V. F. Newcombe, J. P. Simpson, A. D. Kane, D. K. Menon, *et al.*, "Efficient multi-scale 3D CNN with fully connected CRF for accurate brain lesion segmentation," *Medical image analysis,* vol. 36, pp. 61-78, 2017.

[76] J. Zilly, J. M. Buhmann, and D. Mahapatra, "Glaucoma detection using entropy sampling and ensemble learning for automatic optic cup and disc segmentation," *Computerized Medical Imaging and Graphics,* vol. 55, pp. 28-41, 2017.

[77] M. Abdel-Basset, V. Chang, H. Hawash, R. K. Chakrabortty, and M. Ryan, "FSS-2019-nCov: A deep learning architecture for semi-supervised few-shot segmentation of COVID-19 infection," *Knowledge-Based Systems,* vol. 212, p. 106647, 2020.

[78] Q. Chen, Y. Zhao, Y. Liu, Y. Sun, C. Yang, P. Li, *et al.*, "MSLPNet: multi-scale location perception network for dental panoramic X-ray image segmentation," *Neural Computing and Applications,* pp. 1-15, 2021.

[79] W. Ding, M. Abdel-Basset, H. Hawash, and W. Pedrycz, "Multimodal Infant Brain Segmentation by Fuzzy-informed Deep Learning," *IEEE Transactions on Fuzzy Systems*, 2021.

[80] W. H. Pinaya, A. Gadelha, O. M. Doyle, C. Noto, A. Zugman, Q. Cordeiro, *et al.*, "Using deep belief network modelling to characterize differences in brain morphometry in schizophrenia," *Scientific reports,* vol. 6, pp. 1-9, 2016.

[81] H. Fu, J. Cheng, Y. Xu, D. W. K. Wong, J. Liu, and X. Cao, "Joint optic disc and cup segmentation based on multi-label deep network and polar transformation," *IEEE transactions on medical imaging,* vol. 37, pp. 1597-1605, 2018.

[82] J. Zhang, Y. Xie, Q. Wu, and Y. Xia, "Medical image classification using synergic deep learning," *Medical image analysis,* vol. 54, pp. 10-19, 2019.

[83] W. Wang, D. Liang, Q. Chen, Y. Iwamoto, X.-H. Han, Q. Zhang, *et al.*, "Medical image classification using deep learning," in *Deep Learning in Healthcare*, ed: Springer, 2020, pp. 33-51.

[84] Y. Guo and A. S. Ashour, "Neutrosophic multiple deep convolutional neural network for skin dermoscopic image classification," in *Neutrosophic Set in Medical Image Analysis*, ed: Elsevier, 2019, pp. 269-285.

[85] F. Özyurt, E. Sert, E. Avci, and E. Dogantekin, "Brain tumor detection based on Convolutional Neural Network with neutrosophic expert maximum fuzzy sure entropy," *Measurement,* vol. 147, p. 106830, 2019.

[86] N. E. M. Khalifa, F. Smarandache, G. Manogaran, and M. Loey, "A study of the neutrosophic set significance on deep transfer learning models: An experimental case on a limited covid-19 chest x-ray dataset," *Cognitive Computation,* pp. 1-10, 2021.

[87]   G. Cai, Y. Guo, W. Chen, H. Zeng, Y. Zhou, and Y. Lu, "Neutrosophic set-based deep learning in mammogram analysis," in *Neutrosophic Set in Medical Image Analysis*, ed: Elsevier, 2019, pp. 287-310.

[88]   A. I. Shahin and S. Almotairi, "An accurate and fast cardio-views classification system based on fused deep features and LSTM," *IEEE Access*, vol. 8, pp. 135184-135194, 2020.

[89]   I. C. Moreira, I. Amaral, I. Domingues, A. Cardoso, M. J. Cardoso, and J. S. Cardoso, "Inbreast: toward a full-field digital mammographic database," *Academic radiology*, vol. 19, pp. 236-248, 2012.